Applied Geochemistry 49 (2014) 68–76

Contents lists available at ScienceDirect

Applied Geochemistry

journal homepage: www.elsevier.com/locate/apgeochem

Analysis of anion adsorption effects on alumina nanoparticles stability

Tiziana Missana *, Ana Benedicto, Natalia Mayordomo, Ursula Alonso

CIEMAT, Department of Environment, Avenida Complutense, 40, 28040 Madrid, Spain

ARTICLE INFO

Article history:
Available online 16 April 2014

ABSTRACT

Nanoparticles and colloids can be relevant in contaminant migration if the contaminant is strongly adsorbed onto the particles and they are stable and mobile. The main conditions required for a colloidal system to be considered as "*stable*" are: (1) low ionic strength of the groundwater ($\leqslant 1 \times 10^{-3}$ M) and (2) pH far from the point of zero charge (pH_{PZC}). These conditions however, are too simplified to describe the colloidal behaviour in real cases; in fact, specific adsorption of different ions may also have an important impact on colloid stability.

In particular, in this study we analyse the effects of the adsorption of inorganic anions on Al_2O_3 oxide nanoparticles (alumina NPs) stability, combining batch adsorption studies with electrophoretic and dynamic light scattering measurements. Selenite adsorption was studied in a wide range of pHs (3–11), ionic strengths (5×10^{-4} – 1×10^{-1} M) and selenite concentration. Different electrolytes were used to understand the competitive effects for selenite sorption of different anions in solution (ClO_4^-, NO_3^-, HCO_3^-, SO_4^{2-}) and especially their overall influence on alumina NPs stability.

The positive charge of alumina, under acid and neutral-alkaline pHs, favours anion adsorption which, in turn, may result in a decrease of the net surface charge, promoting particle aggregation and the destabilisation of the system. Results showed that, the higher the anion affinity for alumina surface and sites occupancy, the higher the destabilisation of particles. The sorption selectivity observed in our study was: $SeO_3^{2-} > SO_4^{2-} > HCO_3^- > NO_3^- > ClO_4^-$.

Upon anion adsorption, particles aggregation was evident, but a clear change in ζ-potential, was only observed with very high surface occupancies. Surface complexation modelling has been shown to be useful supporting tool for stability studies.

1. Introduction

Amongst the most interesting colloidal particles from an environmental point of view are: oxy-hydroxides and clay minerals that are ubiquitous in groundwater (Sen and Khilar, 2006). Furthermore, with a rising demand for their application, nano-oxides are candidates for multiple industrial uses and therefore their release to the environment, leading to possible harmful effects, is likely.

Under favourable chemical-physical conditions, colloids and nanoparticles (NPs) can travel large distances; thus their migration is of special interest when these particles may carry some type of contaminant. Many uncertainties still exist on colloid-driven contaminant transport and this is an issue of concern associated to hazardous waste repositories (Geckeis, 2004). NPs and colloids may enhance contaminant transport in groundwater, provided the contaminant is irreversibly adsorbed onto their surface and the particles are stable and mobile (McCarthy and Zachara, 1989; Miller et al., 1994; Sen and Khilar, 2006, and references therein). The kinetics of processes and residence times play also a very important role in colloid transport thus, under certain conditions, NPs may enhance contaminant migration even its sorption onto the particle surfaces is (partially) reversible.

Surface properties mostly determine colloidal behaviour in terms of stability, mobility and ion adsorption, therefore their study is fundamental. Furthermore, changes in particle size upon aggregation alter colloid transport properties, their reactivity, toxicity and bioavailability. Furthermore, speciation of colloids through the whole transport system should be considered.

In general, oxide colloids are stable and more mobile, when the ionic strength of the groundwater is low ($\leqslant 1 \times 10^{-3}$ M) and the pH is far from the point of zero charge (pH_{PZC}). Some parameters like the critical coagulation concentration, CCC, the pH_{PCZ} or the isoelectric point (pH_{IEP}) are normally used to define the stability of colloidal systems. Nevertheless, these parameters are usually determined in simplified systems and using indifferent (non-sorbing) electrolytes; for this reason, sometimes, they are not totally representative of the real behaviour of colloids in nature.

In particular, it is well known that specific adsorption of different ions may have an important impact on colloid stability (Stumm

* Corresponding author. Tel.: +34 913466140.
E-mail address: tiziana.missana@ciemat.es (T. Missana).

http://dx.doi.org/10.1016/j.apgeochem.2014.04.003
0883-2927/

et al., 1970). The CCC of a colloidal system is inversely proportional to the n^{th} power of the counterion (Schulze and Hardy rule) but it decreases if the ions in solution are sorbing (Stumm et al., 1970). This means that sorbable ions may destabilize colloid at much lower concentration that inert ions. This is a very important point because DLVO theory, which is widely used to assess the stability of colloidal particles, mostly neglects the dominating role that chemical forces may play in a system.

The description of the colloidal behaviour under real conditions deserves more in-depth analyses. Additionally, as the adsorption itself could modify surface colloid properties, the effects of ion adsorption on colloid stability are of special interest, for example, when colloid-driven contaminant migration is analysed (Benedicto et al., 2013). In this special case, it is necessary to understand under what conditions these surface modifications may occur, and if these modifications could enhance or inhibit contaminant transport.

In regard to colloid stability, the effects of organic anions or polyelectrolyte are largely documented. The stability of alumina NPs in the presence of natural organic matter was studied by Ghosh et al. (2008). In general, organic coatings are reported to increase substantially colloidal stability: these coatings impart negative charge masking the surface properties of the original particles and dominate interface reactions (Tiller and ÓMelia, 1993; Tipping and Higgins, 1982; O'Melia and Tiller, 1993; Illes and Tombacz, 2006). Tombacz et al. (1999) studied the influence of humate, gallate, salicylate onto clays and aluminium oxide at pH 7–8, in the presence of indifferent electrolytes. Under these conditions, they observed an increased stabilization of the oxide in the presence of relatively small quantities of organic ions. Other polyelectrolytes were also capable of modifying the surface properties of oxides and increase their stability (Singh et al., 2005; Puls et al., 1993; Liang and Morgan, 1990). In any case, the degree of stabilization (or destabilization) of the colloids depends on their point of zero charge and the specific interactions occurring.

On the other hand, the (potentially relevant) effects of inorganic anions present in solution on colloid stability are mostly neglected. Evaluating methods of preparation of aluminium oxide monodispersed suspensions, Brace and Matjevic (1973) already observed large effects of the presence of sulphate on the surface charge of the particles and their pH_{PZC}. But although many studies on adsorption on oxy-hydroxides of inorganic anions (carbonate, phosphate, sulphate, selenite/selenate arsenic) and competitive effects between them exist (Zhang and Sparks, 1990; Balistrieri and Chao, 1987; Peak, 2006; Missana et al., 2009; Wu et al., 2000, 2002; Yamani et al., 2014; Katai et al., 2012; Loffredo et al., 2011; Kim et al., 2004), the effects of inorganic anion adsorption on the stability of colloid has been scarcely reported. Chorover et al., 1997, reported the effects of phosphate adsorption on hematite coagulation; more recently, Benedicto et al. (2013) analysed the variations of TiO_2 nanoparticle size distribution, caused by selenite adsorption, and suggested the importance of studying contaminant adsorption onto colloids and their aggregation behaviour in an integrated form, to assess the potential of colloid-facilitated migration.

The main aim of this study is to evaluate the effects of the adsorption of inorganic anions on Al_2O_3 nanoparticle (alumina NPs) stability. This will show the importance of considering inorganic anions to assess the stability of a colloidal system in natural waters. The analysis will be done combining batch adsorption studies, electrophoretic and dynamic light scattering techniques being the combination of different techniques fundamental. Furthermore, as ion adsorption significantly affects nanoparticle stability, the use of (mechanistic) sorption models will be shown to be very useful tool for supporting stability studies.

Selenite is the main anion analyzed, and its adsorption is studied using different electrolytes, to verify the adsorption strength other anions (through competitive effects with selenium) and their possible relevance on the oxide stability. Selenium is introduced in the environment from both natural and anthropogenic sources mainly combustion of fossil fuels, disposal of fly ash, mining activities and agriculture. It is an element of special concern also in the frame of nuclear waste repository for the long-life of the ^{79}Se isotope and its high mobility. The effects of selenite adsorption, on alumina NPs stability, have been studied in a wide range of selenite concentrations as to cover different possible contamination scenarios.

The pH_{PZC} of alumina, as widely reported in the literature (Ghosh et al., 2008; Kosmulski, 2009a,b; Huang and Stumm, 1973; Sverjenski and Sahai, 1996; Schulthess and Sparks, 1986; Westall and Hohl, 1980) is in the alkaline range (pH = 8.0–9.5); thus, the oxide presents positive charge in a wide range of pH and it is quite appropriated for studying anion adsorption. Additionally, alumina surface functional groups resemble those present at the edge of clay particles (aluminols), so this study can also help understanding the stability of natural clay colloids in natural systems, in the presence of inorganic anions.

2. Materials ad methods

2.1. Nanoparticles

The nanoxide used in this work was alumina powder (Al_2O_3, CAS 1344-28-1) provided by Aldrich, with a particle nominal size <50 nm. The N_2-BET specific surface area is 136 m^2/g. For stability and sorption experiments, the oxide was directly suspended in different electrolytes at the desired solid to liquid ratio and put in the ultrasound during 1 h, before the measurements.

The mean size of dried particles was analyzed by AFM. The AFM samples were prepared suspending the oxide (116 ppm) in deionized water at two different pH values (4.5 and 6.5). A drop of these suspensions was deposited onto a freshly cleaved mica substrate and dried in an oven at 60 °C. Fig. 1 shows the AFM image obtained with the sample prepared at pH 6.5, which confirms that the primary particles have a mean size <50 nm. Aggregates with a size around 100–200 nm are also visible. Both the size and the shape of the particles are not homogeneous. Similar images were obtained with the sample prepared at pH 4.5.

2.2. Selenium

The tracer used for sorption experiments was a carrier-free ^{75}Se (as H_2SeO_3 (selenite) in 0.1 HCl, Isotope Products). Most ^{75}Se

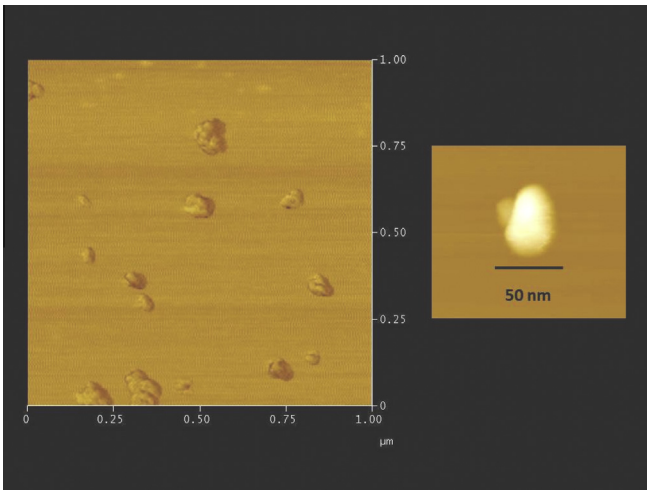

Fig. 1. AFM image (tapping mode) of the alumina nanoparticles, prepared at pH 6.5. In the right part of the figure a detail of a single particle is shown.

radiation is in the form of gamma emissions at 136 and 265 keV. The half-life of ^{75}Se is 119.8 days. Selenium activity in solution was measured by γ-counting with a NaI detector (Packard Autogamma COBRA 2).

In the experiments to evaluate nanoparticle stability upon selenite adsorption, Se concentrations higher than 1×10^{-6} M were obtained using a non-radioactive chemical (Na_2SeO_3) of high purity (Aldrich).

2.3. Sorption experiments

Batch sorption experiments were carried out under atmospheric conditions. Suspensions of 0.5 g/L of alumina powder in different electrolytes and various ionic strengths (I) were used. The electrolyte concentration varied from 5×10^{-4} M to 1×10^{-1} M in $NaClO_4$ and it was fixed to 1×10^{-3} in $NaNO_3$, $NaHCO_3$ and Na_2SO_4. The concentration of approximately 10^{-3} M is representative of the possible anion content in natural groundwaters: furthermore, the low ionic strength is selected to maintain, in principle, colloid stability.

The *kinetics* of the sorption process was first investigated to determine the time needed to reach the sorption steady-state. Kinetic tests were carried out at pH 5–6 and an ionic strength of 1×10^{-1} M. One week was considered enough to perform the rest of sorption tests. In particular, *sorption edges* (i.e. sorption curves as a function of pH) were carried out varying the pH of the suspensions from approximately pH 3 to 11.

Depending on the electrolytes used, 0.1 or 1 M $HClO_4$, HNO_3, H_2CO_3 or H_2SO_4 were used to acidify the samples; NaOH was always used as a base. Measurements of pH (±0.10) were made using a combined glass pH electrode (Metrohm) that incorporated an Ag/AgCl reference electrode. The electrode was calibrated using buffer solutions (Scharlau) at pH 4.00, 7.00 and 10.00.

In sorption experiments, the traced suspensions ([^{75}Se(IV)]$\sim 5.8 \times 10^{-7}$ M) were introduced in 12 mL polypropylene tubes. The solid and liquid phases were separated by centrifuging (23,000*g* for 1 h). After the solid separation, three aliquots of the supernatant were extracted from each tube for the analysis of the final activity.

The distribution coefficient for the solid and the liquid phase, K_d, was calculated with this formula:

$$K_d = \frac{C_i - C_f}{C_f} \cdot \frac{V}{m} \quad (1)$$

C_i and C_f are the initial and final concentration of selenium in the liquid phase (Bq·mL^{-1}), m the mass of the clay (g) and V the volume of the liquid (mL).

Sorption onto the vials and ultracentrifuge tubes was measured after sorption experiments. Selenium sorption onto these vessels was always negligible (<2%), therefore it was not accounted for in K_d calculations.

2.4. Alumina nanoparticles surface charge and stability

The stability of alumina NPs as a function of electrolyte pH and ionic strength as well as selenium (and other electrolyte anions) adsorption was evaluated studying their surface potential and measuring their mean size upon the induced chemical change.

Nanoparticles surface charge was analysed by potentiometric titrations and the measurement of their ζ-potential. Potentiometric titrations were carried out using 10 g/L of alumina suspended in $NaClO_4$ at two different ionic strengths (1×10^{-1} and 1×10^{-2} M), in a glove box with N_2 atmosphere to avoid CO_2 contamination.

The ζ-potential was measured by means of the laser Doppler electrophoresis technique using a Malvern Zetamaster apparatus equipped with a 5-mW He–Ne laser ($\lambda = 633$ nm), using alumina suspensions of 50–100 ppm. The ζ-potential was calculated from the measured electrophoretic mobility using the Smoluchowski equation (Smoluchowski, 1921; Jiang et al., 2009; Kosmulski, 2009a, 2009b).

The mean particle size was measured by photon correlation spectroscopy (PCS), that is the most well-developed and commonly used technique for hydrodynamic size measurement (Jiang et al., 2009). PCS technique applies the Stokes–Einstein equation for the mean hydrodynamic diameter calculation, from the measured temporal evolution of the scattered light by particles under Brownian motion (Jiang et al., 2009).

PCS measurements were carried out with a 4700 Malvern apparatus equipped with a Spectra Physics 4-W argon laser ($\lambda = 514$ nm) and a Malvern 7032 digital autocorrelator. The photomultiplier was located at 90° with respect to the laser beam incident in the sample. In some cases, the mean particle size was measured with a ZetaSizer Nano ZS (Malvern) available in the radioactive laboratory (He-Ne laser, $\lambda = 633$ nm, photomultiplier at 173°). The concentration of the alumina NPs in the samples used for size measurements was 50–100 ppm.

2.5. Modelling

Oxide–water interface was widely described in the past (Dzombak and Morel, 1990; Huang and Stumm, 1973): the surface of inorganic oxides in aqueous environment displays reactive sites of amphoteric character (SOH), able to undergo a variety of physico-chemical processes. Ion adsorption on oxide surfaces occurs by complexation on these sites.

These amphoteric groups react with hydroxyl ions (Stumm and Morgan, 1981; Sposito, 1984) producing a pH-dependent surface charge defined by the following reactions:

$$SOH_2^+ \Longleftrightarrow SOH + H^+ \quad K_{a1} \quad (2)$$

$$SOH \Longleftrightarrow SO^- + H^+ \quad K_{a2} \quad (3)$$

where SOH_2^+, SOH and SO^- represents, respectively, the positively charged, neutral and negatively charged surface sites; and K_{a1} and K_{a2} are the intrinsic equilibrium acidity constants. The mass law equations corresponding to the reactions (2) and (3) are the following:

$$K_{a1} = \frac{(SOH)\{H^+\}}{(SOH_2^+)} \exp\left(-\frac{F\Psi}{RT}\right) \quad (4)$$

$$K_{a2} = \frac{(SO^-)\{H^+\}}{(SOH)} \exp\left(-\frac{F\Psi}{RT}\right) \quad (5)$$

where {} represents the ion activity and () the ion concentrations. Because the activity coefficients for all the surface species are assumed to be equal, the activity of these species can be substituted by their concentration (). The exponential function represents the columbic term that accounts for the electrostatic effects. Non-electrostatic models, such as that used in our work, do not consider this correction.

Anion adsorption onto SOH sites can be described with reactions of this type:

$$SOH + H^+ + A^{n-} \Longleftrightarrow SA^{(n-1)-} + H_2O \quad K_c \quad (6)$$

where A is the hypothetical anionic species.

Standard thermodynamic data, from Séby et al. (2001), were used to calculate selenium speciation. Under our experimental conditions, selenite speciation calculations show that from pH 3 to 8.5, the predominant specie is $HSeO_3^-$, and for a pH above 8.5 the main specie is SeO_3^{2-}. Therefore the main reactions considered

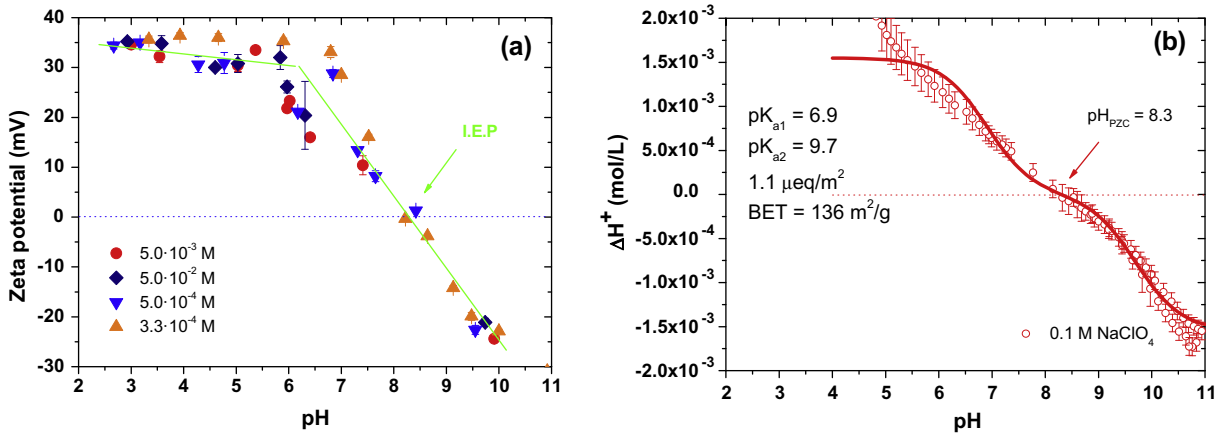

Fig. 2. (a) ζ-Potential of the alumina NPs in $NaClO_4$ at four different ionic strengths (I); (b) potentiometric titration curve of the alumina in $NaClO_4$ 0.1 M and fit with the non-electrostatic model.

in this study to describe selenite adsorption on the alumina NPs surface will be:

$$SOH_2^+ + SeO_3^{2-} \Longleftrightarrow SOH_2SeO_3^- \quad K_{cSe1} \tag{6a}$$

and

$$SOH_2^+ + HSeO_3^- \Longleftrightarrow SOH_2HSeO_3^0 \quad K_{cSe2} \tag{6b}$$

The formation of these two surface species was previously proposed by various studies of selenite sorption onto aluminium and iron oxides (Balistrieri and Chao, 1990; Duc et al., 2003, 2006; Zhang and Sparks, 1990; Goldberg, 1985; Parida et al., 1997; Missana et al., 2009).

Calculations showed that selenite might undergo oxidation at pHs higher than 8, allowing the coexistence of selenite and selenate in this region (Benedicto et al., 2013). In any case, this would not be an especially relevant issue for the scopes of the present study and redox processes were not accounted for.

The modelling calculations were performed with the CHESS v 2.4 code (van der Lee and de Windt, 1999) and the fit of the experimental curves were obtained with a trial and error procedure. The adsorption of the electrolyte anion was taken into account including the corresponding Eq. (6) for each anion coexisting in solution (ClO_4^-, SO_4^{2-}, NO_3^- or HCO_3^-):

$$SOH_2^+ + ClO_4^- \Longleftrightarrow SOH_2ClO_4 \tag{6c}$$

$$SOH_2^+ + HCO_3^- \Longleftrightarrow SOH_2HCO_3 \tag{6d}$$

$$SOH_2^+ + NO_3^- \Longleftrightarrow SOH_2NO_3 \tag{6e}$$

$$SOH_2^+ + SO_4^{2-} \Longleftrightarrow SOH_2SO_4^- \tag{6f}$$

3. Results and discussion

3.1. Surface charge and potential of alumina nanoparticles

The ζ-potential of the alumina NPs as a function of pH and at four different ionic strengths (5×10^{-2}, 5×10^{-3}, 5×10^{-4} and 3.3×10^{-4} M in $NaClO_4$) is shown in Fig. 2a. Results showed that the ζ-potential does not depend significantly on the ionic strength and that the isoelectric point of the oxide (pH_{IEP}) is near 8.5.

As additional characterisation of the alumina surface, and to determine the pKs of the protonation/deprotonation of alumina NPs surface functional groups for sorption modelling purpose, potentiometric titrations were carried out. Fig. 2b shows the results of the potentiometric titration obtained at 0.1 M $NaClO_4$. Also in titration experiments, data obtained at lower ionic strength (1×10^{-2} M) were similar and therefore the fit of titration curves was carried out considering a non-electrostatic model. The obtained p*K*s for the (de)protonation reactions (Eqs. (2) and (3)) by the fit of the titration curves, were: $pK_{a1} = 6.9$ and $pK_{a2} = 9.7$ (leading to a $pH_{PZC} = 8.3$) and the density of sorption sites was 1.1 μeq/m^2. All these data are summarised in Table 1. Both pH_{IEP} and pH_{PCZ} obtained are in agreement with values previously published in the literature. The density of sorption sites is also comparable to that obtained for alumina in previous works (Westall and Hohl, 1980; Reich and Koretsky, 2011).

3.2. Alumina nanoparticle size and stability

To analyse more in depth the stability of a colloidal system dynamic light scattering techniques are used; they are able to measure the change in the size of the particles, and the kinetic of the

Table 1
Parameters used for the sorption modelling.

BET: 136 m^2/g
Surface site density: 1.1 μeq/m^2

	Reactions	Definition of the species in the CHESS code		
Surface acidity	$SOH_2^+ \Longleftrightarrow SOH + H^+$	SOH_2[+]	1 SOH, 1 H[+]	log*K* = 6.9
	$SOH \Longleftrightarrow SO^- + H^+$	SO[−]	1 SOH, −1 H[+]	log*K* = −9.7
Selenium adsorption	$SOH_2^+ + SeO_3^{2-} \Longleftrightarrow SOH_2SeO_3^-$	SOH_2SeO_3[−]	1 H[+], 1 SOH, 1 SeO_3[2−]	log*K* = 13.30
	$SOH_2^+ + HSeO_3^- \Longleftrightarrow SOH_2HSeO_3^0$	SOH_2HSeO_3	2 H[+], 1 SOH, 1 SeO_3[2−]	log*K* = 21.60
Perchlorate adsorption	$SOH_2^+ + ClO_4^- \Longleftrightarrow SOH_2ClO_4^0$	$SOHClO_4$	1 H[+], 1 SOH, 1 ClO_4[−]	log*K* = 8.5
Nitrate adsorption	$SOH_2^+ + NO_3^- \Longleftrightarrow SOH_2NO_3^0$	$SOHNO_3$	1 H[+], 1 SOH, 1 NO_3[−]	log*K* = 9.5
Bicarbonate adsorption	$SOH_2^+ + HCO_3^- \Longleftrightarrow SOH_2HCO_3^0$	$SOHHCO_3$	1 H[+], 1 SOH, 1 HCO_3[−]	log*K* = 11.5
Sulfate adsorption	$SOH_2^+ + SO_4^{2-} \Longleftrightarrow SOH_2SO_4^-$	$SOHSO_4$[−]	1 H[+], 1 SOH, 1 SO_4[2−]	log*K* = 12.30

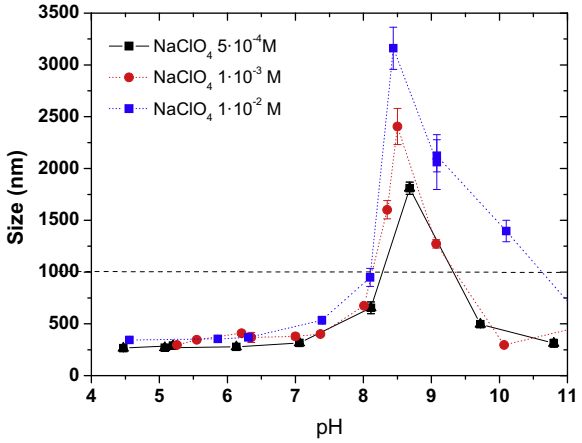

Fig. 3. Size of the alumina NPs as a function of pH at three different ionic strengths in $NaClO_4$: 5×10^{-4} (▲); 1×10^{-3} (●) and 1×10^{-2} (■) M. The lines are drawn to guide the eye.

process, under certain chemical conditions and upon a change in the chemistry.

An increase in particles size indicates that they are aggregating and that the colloidal system is not stable anymore. Stability studies are mainly carried out as a function of the pH and ionic strength of the suspending solution. Oxy-hydroxide particles aggregate near the pH_{PZC}, because, in absence of surface charge, electrostatic repulsion does not exist; and also when the ionic strength (I) of the solution increases. The increase of the ionic strength, causes the shrinking of the electrical double layer of the particles; double layer thickness (κ^{-1}) is inversely proportional to the square root of the ionic strength (I); thus, the increase of I, favours particles approach, their collision and attachment. In spite of that, an increase in ionic strength not always has a clear effect on colloid ζ-potential, as seen in Fig. 2a, for this reason, in this study we want to stress the importance to complement ζ-potential measurements with direct measurements of particle size.

Fig. 3 shows PCS measurements, to determine the size of alumina NPs as a function of the pH and $NaClO_4$ concentration (5×10^{-4}, 1×10^{-3}, 1×10^{-2} M). At the lowest ionic strength and pH far from the point of zero charge, particles are mostly in a disaggregated state. The minimum size of the NPs, measured under these conditions by PCS, is around 280 ± 10 nm, a value higher than that observed by AFM (Fig. 1). PCS technique measures the hydrodynamic size of the particles, which includes the layer of water adhered to the particles surface moving with them, in addition alumina is hygroscopic: these are most probably the reasons why the hydrodynamic size is higher than that measured for the dry oxide by AFM. Furthermore, in PCS measurements, a few larger particles or aggregates can mask the smaller ones, leading to an increased mean hydrodynamic size.

In any case, the value of 280 nm will be considered as the reference hydrodynamic size, for alumina NPs in the *disaggregated* state.

Approaching the pH_{PZC} of the oxide (pH 8.3), the particles clearly aggregate: their mean size significantly increases, with values >1 μm. Increasing the ionic strength, even far from the pH_{PZC}, the mean size of the particle increases, but it remains in the colloidal size.

3.3. Selenite adsorption onto alumina NPS: effects of pH, ionic strength and suspending electrolyte

Fig. 4 shows selenite adsorption on alumina NPs as a function of pH, in different electrolytes. Fig. 4a shows the results obtained in $NaClO_4$ at different ionic strengths (5×10^{-4}, 5×10^{-3}, 5×10^{-2} and 1×10^{-1} M) and Fig. 4b those obtained in other suspending electrolytes ($NaNO_3$, Na_2SO_4 and $NaHCO_3$) at the concentration of 1×10^{-3} M. In all the cases, Se(IV) adsorption decreases with pH, as expected for anions. Under acidic conditions, a slight dependence of sorption on ionic strength is observed (Fig. 4a). This dependence could be related to the formation of outer sphere complexes, or to the adsorption of ClO_4^- that would compete with selenite for sorption sites.

In many studies, author states that the coexistence of outer sphere and inner sphere selenite complexes cannot be discarded (Peak, 2006), even if the main mechanisms of selenite complexation into oxides is inner-sphere (Goldberg et al., 2007). Therefore inner sphere complexes will be considered in this study to interpret selenite sorption data, but possible competitive effects, due to the presence electrolyte anions, will be considered.

Fig. 4b, clearly shows that, when the electrolyte is Na_2SO_4, selenite adsorption is much lower in all the pH range, in agreement with a strong competition of SO_4^{2-} for selenite adsorption onto alumina NPs sites. Selenite sorption onto alumina NPs is quite similar in $NaClO_4$ and $NaNO_3$; in the case of $NaHCO_3$, the shape of the sorption edge is different, possibly indicating a different pH-dependent competitive effect, caused by carbonate speciation.

Experimental sorption data presented in Fig. 4, were simulated using a non-electrostatic model, including both reactions 6a and 6b for selenite complexation and, depending on the suspending electrolyte ($NaClO_4$, $NaHCO_3$, $NaNO_3$ and Na_2SO_4) the corresponding reaction, as described in paragraph 2.5.

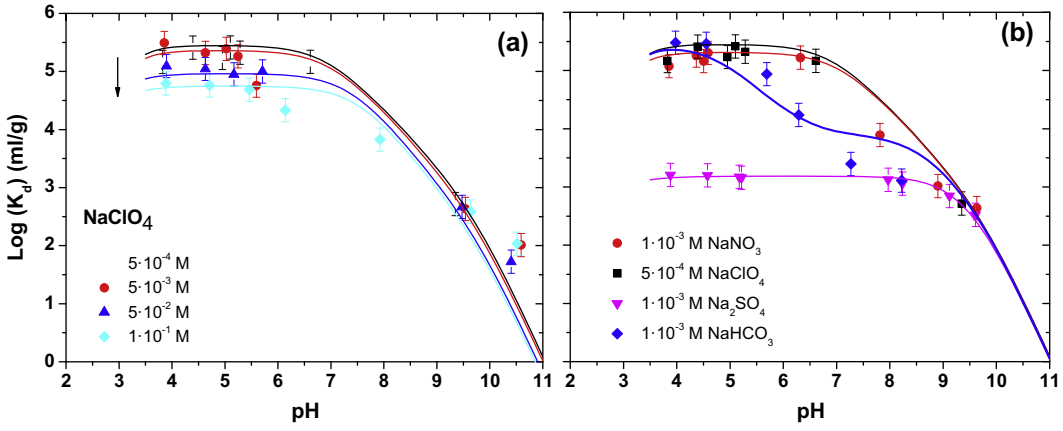

Fig. 4. Selenite adsorption on alumina NPs as a function of pH in different electrolytes. (a) In $NaClO_4$ at different concentrations and (b) in other electrolytes at a concentration of 1×10^{-3} M. Continuous lines correspond to the sorption model obtained with the parameters of Table 1.

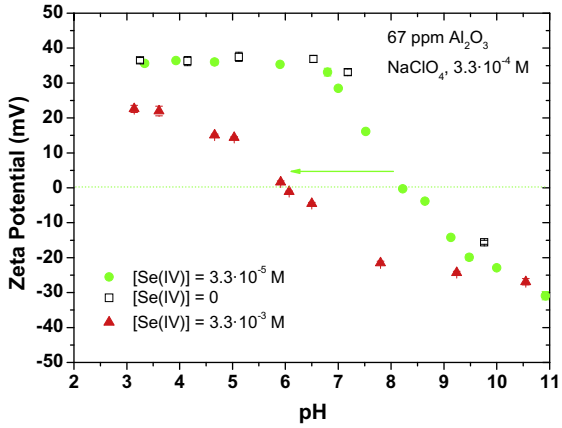

Fig. 5. Zetapotential of alumina NPs suspended in $NaClO_4$ 3.3×10^{-4} as a function of the pH with: [Se] = 0; [Se] = 3.3×10^{-5} M and [Se] = 3.3×10^{-3} M.

The results of the modelling are superimposed to the experimental data in Fig. 4, as continuous lines. The parameters used for the fit are summarised in Table 1. It is clear that the most competitive ion for selenite sorption is SO_4^{2-}, thus indicating stronger affinity of SO_4^{2-} for the alumina surface than the other electrolyte anions. The less competitive anions are: ClO_4^- and NO_3^-; HCO_3^- also clearly affects selenite sorption and causes a different shape of the sorption edge.

The focus of this study is related to the affections of adsorption on NPs colloidal properties, therefore surface complexation modelling will be mainly used as a tool to quantify contaminant adsorption under different chemical conditions and to understand the stability behaviour of alumina NPs in the presence of sorbing anions.

3.4. Alumina nanoparticle stability upon anion adsorption

The central part of this study is to evaluate if anion adsorption affects the stability of the particles: therefore, the surface potential

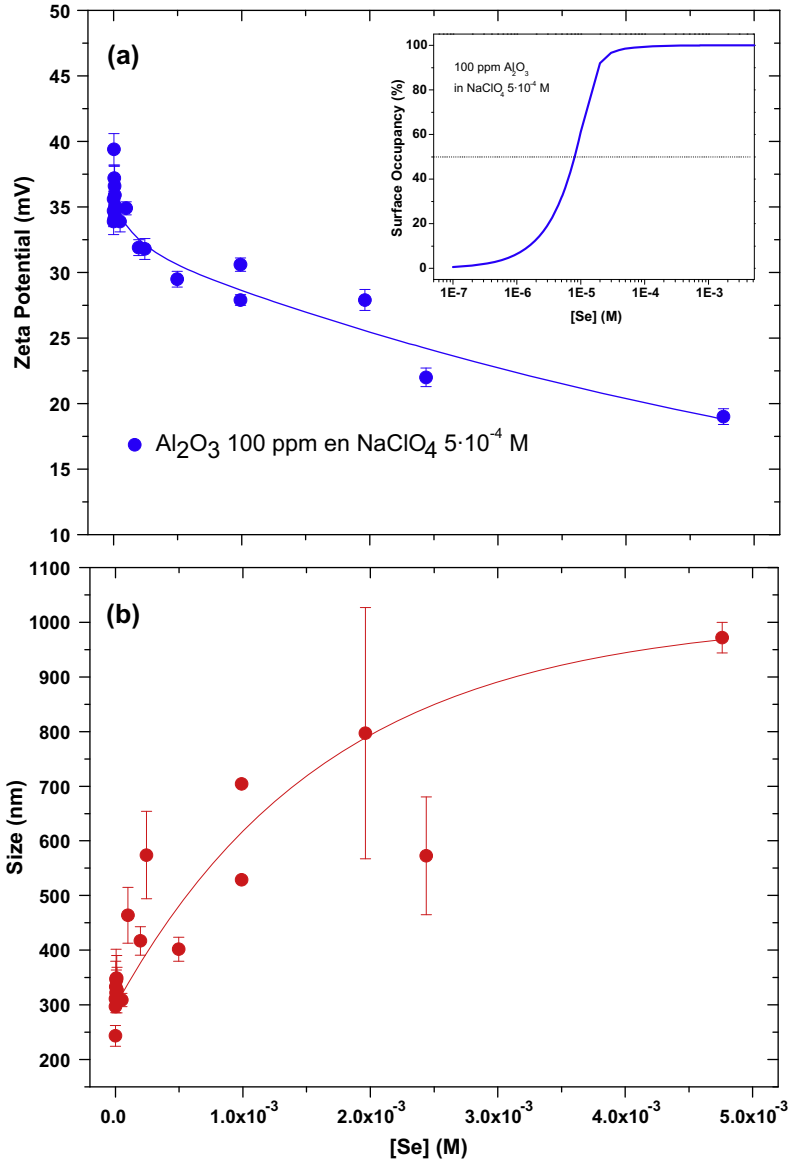

Fig. 6. (a) Zetapotential and (b) mean size of alumina NPs suspended in $NaClO_4$ 5×10^{-4} and pH 4.5 as a function of the [Se(IV)] concentration. In the inset of Fig. 6a, the percentage of alumina surface coverage is shown, calculated with the parameters of the sorption model in Table 1.

and size of alumina NPS will be measured in the presence of different anions.

Fig. 5 shows the ζ-potential of 67 ppm alumina in 3×10^{-4} M $NaClO_4$, as a function of pH, with three different Se(IV) concentrations: 0, 3×10^{-5} M and 3×10^{-3} M. The adsorption up to 3×10^{-5} M of Se(IV) does not change significantly the ζ-potential of the oxide, but increasing Se(IV) to 3×10^{-3} M a clear decrease of the ζ-potential occurs under acidic and slightly alkaline pH; a clear shift towards acidic pH of the pH_{IEP} (pH 6) is also observed. A concentration of approximately 1×10^{-3} M of selenite clearly affects the surface properties of the alumina NPs: according to ζ-potential values, their stability may improve at pH 8–10; remain unvaried at pH > 10 and get worse at pH < 8. Therefore, the range of pH in which alumina NPs are stable in the presence of selenite is smaller than that of alumina alone.

In order to better evaluate the effect of selenite adsorption onto initially stable alumina NPs, we added increasing selenite concentrations to 100 ppm of an alumina suspension in $NaClO_4$ 5×10^{-4} M at pH 4.5 (initial size ~300 nm). Fig. 6a shows the ζ-potential and Fig. 6b shows the mean hydrodynamic size as a function of the selenite added.

The increase of selenite in the suspension, produces a decrease in the ζ-potential, but significant (>10–15 mV) variation was observed only when the added selenite concentration was around $1–3 \times 10^{-3}$ M (Fig. 6a), in agreement with data presented in Fig. 5. The inset of Fig. 6a shows the percentage of sites occupied by selenite, as a function of the initial selenite concentration. Calculations were made considering the data used for sorption modelling, presented in Table 1. According to calculations, the adsorption of selenite of an initial concentration of 3.3×10^{-5} would be around a 96%; this value is still not enough to produce evident changes in ζ-potential, which are observed only with selenite surface occupancy of about 100%.

Nevertheless, the effect on particle aggregation is clearly appreciable at lower selenite concentrations (1–1.5 orders of magnitude less). A substantial increase of the mean hydrodynamic size is observed since the very first selenite additions (Fig. 6b). These results indicate again that, only the measurement of the ζ-potential, is not enough to assess the real stability behaviour of alumina NPs interacting with anions.

Specific adsorption of selenite clearly promotes alumina particle aggregation (Fig. 6b), thus it is interesting observing the effects of other anions, which have been shown, in a certain extent, to interact with the surface of the particles. This is especially interesting for sulphate, which has been observed to significantly sorb onto alumina NPs and considering that concentrations of $1 \times 10^{-4} - 1 \times 10^{-3}$ M of this ion, are not uncommon in natural waters.

Fig. 7 shows the ζ-potential (Fig. 7a) and the mean hydrodynamic size (Fig. 8b) of the alumina NPs suspended in different electrolytes ($NaNO_3$, $NaClO_4$, $NaHCO_3$ and Na_2SO_4) at the ionic strength of 1×10^{-3} M and as a function of pH.

As shown in Fig. 7a, the ζ-potentials on alumina NPs suspended in $NaClO_4$, $NaNO_3$, $NaHCO_3$ are similar, with a pH_{IEP} around 8–8.5. The ζ-potentials of the particles in the presence of Na_2SO_4 is clearly lower and the isoelectric point is also shifted towards pH 7. Again, size measurements give more information on the stability of the particles, as shown in Fig. 7b, where data related of alumina suspended in Na_2SeO_3 ($I = 1 \times 10^{-3}$ M) were also added.

Taking as reference the values obtained with $NaClO_4$, it can be observed that the peak around the pH_{PZC} is broadened in the region towards acidic pHs for all the other electrolytes. This indicates that under acidic conditions the presence of certain anions clearly destabilize alumina NPs. At pH > 9 smaller effects are seen. The degree of induced aggregation increases in this order: $ClO_4^- < NO_3^- < HCO_3^- < SeO_3^{2-} \sim SO_4^{2-}$.

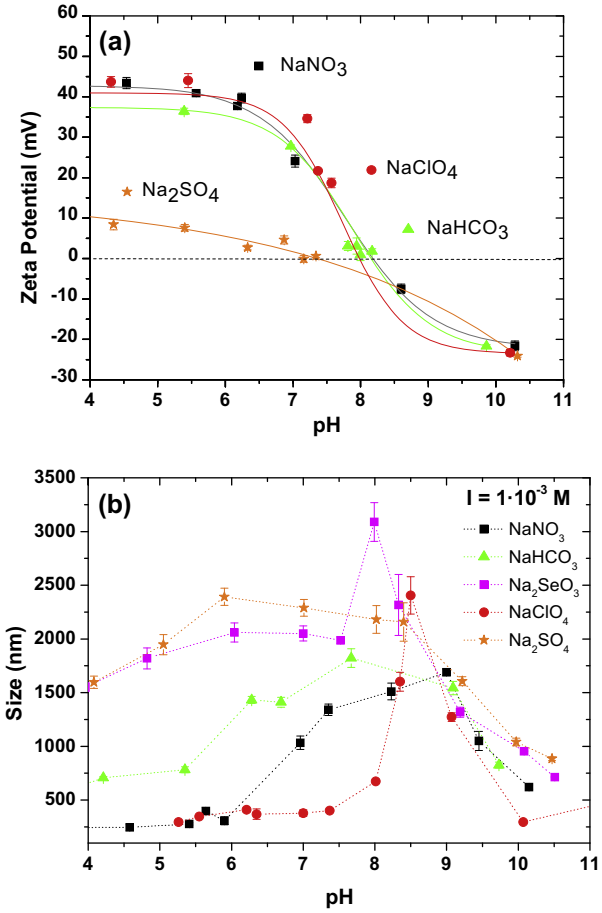

Fig. 7. (a) Zetapotential and (b) mean size of alumina NPs as a function of pH suspended in different electrolytes at $I = 1 \times 10^{-3}$ M.

The capability for anions of destabilizing alumina particles must be related to their adsorption: this has to be evaluated under different chemical conditions and, for this reason, sorption modelling is a very adequate tool supporting stability studies.

Fig. 8 shows the percentage of surface occupancy for alumina NPs, as a function of the pH after the adsorption of electrolyte anions (ClO_4^-, NO_3^-, HCO_3^-, SO_4^{2-}, SeO_3^{2-}), under the experimental conditions described in Fig. 7b (100 ppm of alumina and

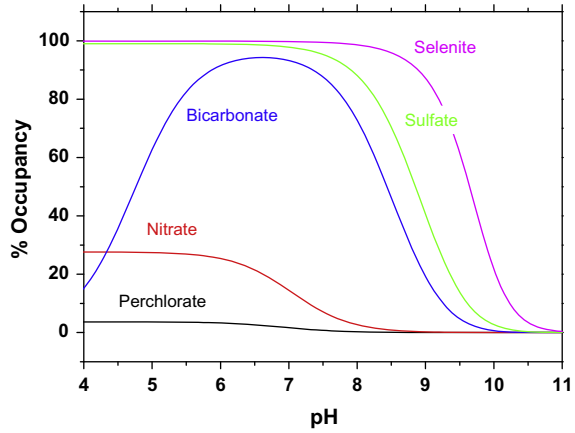

Fig. 8. Calculated percentage of surface occupancy, for each anion, as a function of the pH after the adsorption. Calculations are done considering the experimental conditions of Fig. 7b.

$I = 1 \times 10^{-3}$ M). The calculations were performed using the parameters of the sorption model summarised in Table 1.

The highest surface occupancies upon sorption are always given by selenite and sulfate, with values near to 100% at pH < 7. With this value of surface occupancy, particles are aggregated (Fig. 7b) and modifications are also detected in ζ-potential values (Fig. 7a). However, less concentration of anions at the surface is actually capable of aggregating alumina NPs. Fig. 8 shows that in the presence of HCO_3^- at acidic pH, the surface occupancy for HCO_3^- is variable, however alumina NPs are always in aggregated state. Nevertheless, no changes in ζ-potential are detected. These results evidence the importance of directly checking the aggregation state of the NPs and do not rely only on ζ-potential variations. The comparison between Fig. 7b and the calculations shown in Fig. 8 suggests also that the size of aggregates could depend on the surface occupancy.

4. Conclusions

The stability of alumina NPs was analyzed in the presence of different electrolytes to assess the effects of anion adsorption. Selenite adsorption has been studied as a function of pH, ionic strength and the presence of different anions in solution and experimental data were fit using a non-electrostatic model, considering the competition of the anions of the electrolyte.

Stability studies showed that the presence of highly sorbing anions like selenium and sulphate clearly affects the stability of Al_2O_3 colloids at relatively low concentrations (1×10^{-4} M), even when changes in ζ-potential are not evident. At ionic strength of 1×10^{-3} M and below the point of zero charge (pH < 7) a different aggregation state is observed depending on the electrolyte ($ClO_4^- < NO_3^- < HCO_3^- < SO_4^{2-} \sim SeO_3^{2-}$). This aggregation state is related to the adsorption of the anion and the sorbate surface coverage. Surface complexation modelling has been shown to be an adequate tool to quantify ion adsorption and NPs surface occupancies, under changing chemical conditions, providing insight on the stability behaviour of colloids in the presence of sorbing ions.

In a transport scenario, it is important to follow colloid speciation thorough the whole migration path. In particular the modifications of the particle size (aggregation/disaggregation) are very important, because the size controls Brownian motion, filtration, retention and settling phenomena (Degueldre et al., 2009) and lead to different types of interactions with the host rock and, in the end, different fate of colloids in groundwater.

The results presented in this study show that the presence of anions, frequently obviated in stability studies, must be accounted for, as well as the role that chemical forces may play in a system, otherwise assessments on colloid stability and colloid-driven contaminant transport in the environment might be strongly biased.

Acknowledgements

The research leading to these results has received funding from EU Seventh Framework Programme (FP7/2007-2011) under the Grant Agreement No. 295487 (BELBAR, Bentonite Erosion: effects on the Long term performance of the engineered Barrier and Radionuclide Transport) and the Project the Spanish Ministry of Economy and Competiveness through the NANOBAG Project (CTM2011-27975).

References

Balistrieri, L.S., Chao, T.T., 1987. Selenium adsorption by goethite. Soil. Sci. Soc. Am. 51, 1145–1151.
Balistrieri, L.S., Chao, T.T., 1990. Adsorption of selenium by amorphous iron oxydroxides and manganese dioxide. Geochem. Cosmochim. Acta 54, 739–751.
Benedicto, A., Missana, T., Degueldre, C., 2013. Predictions of TiO_2-driven migration of Se(IV) based on an integrated study of TiO_2 colloid stability and Se(IV) surface adsorption. Sci. Total Environ. 449, 214–222.
Brace, R., Matjevic, E., 1973. Aluminium hydrous oxide sols I – Spherical particles of narrow size distribution. J. Inorg., NuclChem. 35, 3691–3705.
Chorover, J., Zhang, J., Aistadi, M.K., Buffle, J., 1997. Comparison of hematite coagulation by charge screening and phosphate adsorption: difference in aggregate structure. Clays Clay Miner. 45 (5), 690–708.
Degueldre, C., Aeberhard, P., Kunze, P., Besso, K., 2009. Colloid generation/elimination dynamic processes: towards a pseudo-equilibrium? Colloids Surf. A 337 (1–3), 117–126.
Duc, M., Lefevre, G., Fedoroff, M., 2006. Sorption of selenite ions on hematite. J. Colloid Interface Sci. 298, 556–563.
Duc, M., Lefevre, G., Fedoroff, M., Jeanjean, J., Rouchaud, J.C., Monteil-Rivera, F., Dumonceau, J., Milonjic, S., 2003. Sorption of selenium anionic species on apatites and iron oxides from aqueous solutions. J. Environ. Radioact. 70, 61–72.
Dzombak, D.A., Morel, F.M.M., 1990. Surface Complexation Modelling. John Wileys and Sons, NY.
Geckeis, H., 2004. Colloid influence on the radionuclide migration from a nuclear waste repository. In: Gieré, R., Stille, P. (Eds), Energy, Waste and the Environment: A Geochemical Perspective, Geological Society, Special Publication 236, London, pp. 529–543.
Ghosh, S., Mashayekhi, H., Pan, B., Bhowmik, P., Xing, B., 2008. Colloidal behaviour of aluminium oxide nanoparticles as affected by pH and natural organic matter. Langmuir 24 (21), 12385–12391.
Goldberg, S., 1985. Chemical modeling of anion competition on goethite using the constant capacitance model. Soil Sci. Soc. Am. J. 49, 851–856.
Goldberg, S., Lesch, S.M., Suarez, D.L., 2007. Predicting selenite adsorption by soil using soil cemical parameters in the constant capacitance model. Geochim. Cosmochim. Acta 71, 5750–5762.
Huang, C., Stumm, W., 1973. Specific adsorption of cations on hydrous gamma-Al_2O_3. J. Colloid Interface Sci. 43, 409–420.
Illes, E., Tombacz, E., 2006. The effect of humic acid adsorption on pH-dependent surface charging and aggregation of magnetite nanoparticles. J. Colloid Interface Sci. 295, 113–123.
van der Lee, J., De Windt L., 1999. CHESS Tutorial and Cookbook. Technical, Report LHM/RD/99/05.
Jiang, J., Oberdörster, G., Biswas, P., 2009. Characterization of size, surface charge, and agglomeration state of nanoparticle dispersions for toxicological studies. J. Nanopart. Res. 11, 77–89.
Katai, R., Sefti, M.V., Jafari, M., Dehaghani, A., Shariflan, S., Ghayyem, M., 2012. Study effect of different parameters on the sulphate sorption onto nano alumina. J. Ind. Eng. Chem. 18 (1), 230–236.
Kim, C.S., Rytuba, J.J., Brown Jr., G.E., 2004. EXAFS study of mercury(II) sorption to Fe- and Al-(hydr)oxides II. Effects of chloride and sulfate. J. Colloid Interface Sci. 270, 9–20.
Kosmulski, M., 2009. Surface Charging and Points of Zero Charge. Boca Ratón.
Kosmulski, M., 2009b. PH-dependent surface charging and points of zero charge. IV Update and new approach. J. Colloid Interface Sci. 337, 439–448.
Liang, L., Morgan, J.J., 1990. Chemical aspects of iron oxide coagulation in water: laboratory stydies and implications for natural systems. Aquat. Sci. 52, 32.
Loffredo, N., Mounier, S., Thiry, Y., Coppin, F., 2011. Sorption of selenate on soils and pure phases: kinetic parameters and stabilisation. J. Environ. Radioact. 102 (9), 843–851.
McCarthy, J.F., Zachara, J.M., 1989. Subsurface transport of contaminants. Environ. Sci. Technol. 23 (5), 496.
Miller, M., Alexander, R., Chapman, N., McKinley, J., Smellie, J., 1994. Natural Analogue Studies in the Geological Repository of Radiactive Waste, Studies in Environmental Science. In: Monograph. Elsevier, vol. 57.
Missana, T., Alonso, U., Scheinost, A., Granizo, N., García-Gutiérrez, M., 2009. Selenite retention by nanocrystalline magnetite: role of adsorption reduction and dissolution/coprecipitation processes. Geochim. et Cosmochim. Acta 73, 6205–6217.
O'Melia, C.R., Tiller, C.L., 1993. Physicochemical aggregation and deposition in aquatic environment. In: Buffle, van Leeuewen, H.P. (Eds.), Environmental Particles, vol. 2. Lewis, Boca Raton, pp. 353–386 (Chapter 8).
Parida, K.M., Gorai, B., Das, N.N., Rao, S.B., 1997. Studies on ferric oxide hydroxides. 3. Adsorption of selenite (SeO_3^{2-}) on different forms of iron oxyhydroxides. J. Colloid Interface Sci. 185, 355–362.
Peak, D., 2006. Adsorption mechanisms of selenium oxyanions at the aluminium oxide/water interface. J. Colloid Interface Sci. 303, 337–345.
Puls, W.P., Paul, C.J., Clark, D.A., 1993. Surface chemical effects on colloid stability and transport through natural porous media. Coll. Surf. A 73, 287–300.
Reich, T.J., Koretsky, C.M., 2011. Adsorption of Cr(VI) on -alumina in the Presence and Absence of CO_2: Comparison of Three Surface Complexation Models.
Schulthess, C.P., Sparks, D.L., 1986. Backtitration technique for proton isotherm modeling of oxide surface. Soil Sci. Soc. Am. J. 50, 1406–1411.
Séby, F., Potin-Gautier, M., Giffaut, E., Borge, G., Donard, O., 2001. A critical review of thermodynamic data for selenium species at 25 °C. Chem. Geol. 171, 173–194.
Sen, T.K., Khilar, K.C., 2006. Review on subsurface colloids and colloid-associated contaminant transport in saturated porous media. Adv. Colloid Interface Sci. 119, 71–96.
Singh, B.P., Menchavez, R., Takai, C., Fuji, M., Takahashi, M., 2005. Stability of dispersion of colloidal alumina particles in aqueous suspensions. J. Colloid Interface Sci. 291, 181–186.

Smoluchowski, M., 1921. In: Graetz, L. (Ed.). Handbuch der Elektrizitat und des Magnetismus, vol. 2. Barth, Leipzig, pp. 366–428.
Sposito, G., 1984. The Surface Chemistry of Soils. Oxford University Press, Oxford.
Stumm, W., Huang, C.P., Jenkins, S.R., 1970. Specific chemical interaction affecting the stability of dispersed systems. Croat. Chem. Acta 42, 223–245.
Stumm, W., Morgan, J.J., 1981. Aquatic Chemistry. John Wiley and Sons, New York.
Sverjenski, D.A., Sahai, N., 1996. Theoretical prediction of single-site surface-protonation equilibrium constants for oxides and silicates in water. Geochim. Cosmochim. Acta 60 (20), 3773–3797.
Tiller, C.L., ÓMelia, C.R., 1993. Natural organic matter and colloidal stability: models and measurements. Colloid Surf. A 73, 89–102.
Tipping, E., Higgins, D.C., 1982. The effect of adsorbed humic substances on the colloid stability of haematite particles. Colloid Surf. A 5 (2), 85–92.
Tombacz, E., Filipcsei, G., Szekeres, M., Gingl, Z., 1999. Particle aggragation in complex aquatic systems. Colloid Surf. A 151, 233–244.
Westall, J., Hohl, H., 1980. A comparison of electrostatic models for the oxide solution interface. Adv. Colloid Interface Sci. 12, 265–294.
Wu, C.-H., Kuo, C.-Y., Lin, C.-F., Lo, S.-L., 2002. Modeling competitive adsorption of molybdate, sulfate, selenate, and selenite using a Freundlich-type multi-component isotherm. Chemosphere 47 (3), 283–292.
Wu, C.-H., Lo, S.-L., Lin, C.-F., 2000. Competitive adsorption of molybdate, chromate, sulfate, selenate, and selenite on gamma – Al_2O_3. Colloids Surf. A 166 (1–3), 251–259.
Yamani, J.S., Lounsbury, A.W., Zimmerman, J., 2014. Adsorption of selenite and selenate by nanocrystalline aluminum oxide, neat and impregnated in chitosan beads. Water Res. 50, 373–381.
Zhang, P., Sparks, D.L., 1990. Kinetics of selenate and selenite adsorption/desorption at the goethite/water interface. Environ., Sci. Technol. 24, 1848–1856.